

533131
13P

REPRINT/IN/08/EWAIVED

A Wind-Tunnel Parametric Investigation of Tiltrotor Whirl-Flutter Stability Boundaries*

David J. Piatak Raymond G. Kvaternik
Research Engineer Senior Research Engineer
NASA Langley Research Center
Hampton, VA

Mark W. Nixon Chester W. Langston Jeffrey D. Singleton
Aerospace Engineer Aerospace Engineer Aerospace Engineer
Army Research Laboratory, Vehicle Technology Directorate
NASA Langley Research Center
Hampton, VA

Richard L. Bennett Ross K. Brown
Research Project Engineer Research Project Engineer
Bell Helicopter Textron, Inc.
Fort Worth, TX

ABSTRACT

A wind-tunnel investigation of tiltrotor whirl-flutter stability boundaries has been conducted on a 1/5-size semispan tiltrotor model known as the Wing and Rotor Aeroelastic Test System (WRATS) in the NASA-Langley Transonic Dynamics Tunnel as part of a joint NASA/Army/Bell Helicopter Textron, Inc (BHTI) research program. The model was first developed by BHTI as part of the J VX (V-22) research and development program in the 1980's and was recently modified to incorporate a hydraulically-actuated swashplate control system for use in active controls research. The modifications have changed the model's pylon mass properties sufficiently to warrant testing to re-establish its baseline stability boundaries. A parametric investigation of the effect of rotor design variables on stability was also conducted. The model was tested in both the on-downstop and off-downstop configurations, at cruise flight and hover rotor rotational speeds, and in both air and heavy gas (R-134a) test mediums. Heavy gas testing was conducted to quantify Mach number compressibility effects on tiltrotor stability. Experimental baseline stability boundaries in air are presented with comparisons to results from parametric variations of rotor pitch-flap coupling and control system stiffness. Increasing the rotor pitch-flap coupling (δ_3 more negative) was found to have a destabilizing effect on stability, while a reduction in control system stiffness was found to have little effect on whirl-flutter stability. Results indicate that testing in R-134a, and thus matching full-scale tip Mach number, has a destabilizing effect, which demonstrates that whirl-flutter stability boundaries in air are unconservative.

INTRODUCTION

Tiltrotor aircraft offer the benefits of the cruising speed and range of a conventional fixed-wing turbo-prop aircraft and the vertical lift capabilities of a helicopter. These benefits are accomplished by employing tilting engine pylons at the wing tips that drive large diameter proprotors providing both vertical lift in helicopter mode and propulsive thrust in cruise mode. A typical tiltrotor can fly twice as fast and several times further than a conventional

helicopter, since tilting the proprotors such that they act as thrusting propellers avoids the adverse aerodynamic effects of helicopter advancing blade compressibility and retreating blade stall. However, limits are imposed on the maximum forward speed of tiltrotor aircraft by an aeroelastic instability known as whirl flutter.

Consider a flexibly-mounted propeller/nacelle combination with rigid, non-flapping blades in which the pitch and yaw motions are coupled due to gyroscopic forces. When perturbed, the system exhibits stable gyroscopic precession in the absence of aerodynamic forces. If the same propeller/nacelle system is immersed in axial flow and perturbed, aerodynamic loads in addition to propulsive thrust are generated by the precession of the propeller. These loads provide the mechanism for the classical whirl-flutter instability of the backward-whirl mode

* Presented at the American Helicopter Society 57th Annual Forum, Washington, DC, May 9-11, 2001. Copyright © 2001 by the American Helicopter Society International, Inc. No copyright is asserted in the United States under Title 17, U.S. Code. The U.S. Government has a royalty-free license to exercise all rights under the copyright claimed herein for Governmental Purposes. All other rights are reserved by the copyright owner.

(Refs. 1 and 2). The fundamental cause of tiltrotor whirl flutter is the same as that for propeller/nacelle whirl-flutter, namely, the aerodynamic loads generated by precession. However, because of the additional flapping degree of freedom introduced by the tiltrotor's gimballed hub, the manner in which the precession-generated aerodynamic loads act on the pylon/wing, and hence promote whirl flutter, is significantly different from that of classical propeller/nacelle whirl flutter. These differences have been thoroughly examined by Kvaternik in Ref. 3. Past studies have shown that tiltrotor whirl-flutter stability is not only effected by pylon mount stiffness and damping, but also the many rotor system design parameters as determined by wind-tunnel and analytical investigations on the Bell XV-3 tiltrotor configuration (Refs. 4 and 5). Because of the many rotor and wing parameters which affect tiltrotor dynamics, testing of aeroelastically-scaled wind-tunnel models has proven to be an effective method of providing researchers and designers with experimental data on specific tiltrotor configurations. This data is essential for validation of analytical predictions of whirl flutter, loads, and vibration.

Tiltrotor aeroelasticity has long been a subject of attention for researchers at NASA-Langley's Transonic Dynamics Tunnel (TDT). Whirl-flutter stability and dynamics of aeroelastic tiltrotor models such as the Bell Model 266, Bell Model 300, and the Grumman Helicat were extensively investigated during testing at the TDT (Refs. 6 and 7). The effects of pitch-flap coupling, flapping hinge offset, wing/pylon natural frequencies, wing aerodynamics, and altitude were identified. Langley-developed whirl-flutter analytical predictions were shown to be in agreement with the measured stability and response behaviors of these wind-tunnel models (Refs. 8 and 9).

In 1984, during development of the JVX tiltrotor design (later to become the V-22), a Bell-Boeing and NASA-Army team conducted two wind-tunnel tests on a semispan aeroelastic model at the TDT to provide experimental data to guide design efforts and validate analytical methods. The first TDT entry was a broad-based study of the JVX preliminary design in which baseline stability and loads data were defined and the impact of wing stiffness, control system stiffness, pitch-flap coupling, and other parameters were determined for the validation of analytical methods. A gimballed, rigid hub was evaluated and whirl-flutter instability conditions of this configuration were found to be significantly lower than design requirements. Also, parametric studies confirmed that pitch-flap coupling is destabilizing and increasing control system stiffness is stabilizing to whirl flutter for this configuration (Refs. 10 and 11). These results helped guide subsequent JVX design efforts to improve aeroelastic sta-

bility.

The second JVX test at the TDT was conducted to evaluate stability boundaries of the model in a configuration that better represented the then current full-scale design. Model updates included wing stiffness changes, pylon mass changes, stiffened blades, and the inclusion of a stiff in-plane, offset coning-hinge hub designed to simulate the proposed coning flexure of the full-scale design. The full-scale coning flexure and model-scale coning hinge were intended to relieve the steady blade bending deflections to thus reduce the destabilizing effect of positive blade pitch-lag coupling (lag back, pitch up) as shown analytically in Refs. 12 and 13 for a stiff in-plane hub. Also, due to the presence of the offset coning-hinge, the effective magnitude of pitch-flap coupling was reduced which had a stabilizing effect on whirl flutter. The results of the second test demonstrated that the stiff in-plane, offset coning-hinge hub significantly improved the aeroelastic stability over the baseline rigid hub (Refs. 10 and 11). However, no parametric studies of control system stiffness or pitch-flap coupling were performed on the coning-hinge configuration.

During later JVX fullspan and semispan aeroelastic model testing at other wind-tunnel facilities, the stiff in-plane hub's coning-hinge became a flexbeam structure to more closely model the full-scale coning flexure. Again, however, no parametric studies of pitch-flap coupling or control system stiffness were carried out on the flexbeam configuration. Since this series of wind-tunnel tests, there have been no experimental studies showing the effects of important rotor design variables on a gimballed, stiff in-plane hub having a coning flexure. Analyses discussed in Refs. 12 and 13 indicate that pitch-lag coupling has a significant effect on tiltrotor whirl-flutter stability, and is affected by rotor design parameters. Therefore, results from previous parametric studies for a rigid hub can be expected to be different for the coning-flexured hub configuration.

Since 1994, a joint Army/NASA/Bell Helicopter Textron Incorporated (BHTI) team has conducted a variety of wind-tunnel and hover tests of a 1/5-size semispan tiltrotor model aimed at addressing aeroelastic technical areas that have the potential for enhancing the civil and military viability of tiltrotor aircraft. The tiltrotor model is known as the Wing and Rotor Aeroelastic Test System (WRATS) and is a modified version of the semispan JVX/V-22 aeroelastic model described in Ref. 11. Research conducted with this model has included testing of a composite-tailored wing to extend the tiltrotor stability boundary (Refs. 14 and 15), tiltrotor vibration reduction via higher harmonic control (Refs. 16 and 17), and active control of ground resonance for a soft in-plane tiltrotor (Ref. 18).

Modifications have been made to the WRATS model which have changed the pylon mass properties from those of past aeroelastic stability studies. These modifications include the replacement of the original electric motor-driven swashplate control system with one that employs high-bandwidth hydraulic actuators for the application of active controls research. Hydraulic servovalves and associated electronic components have also added mass to the pylon. While attempts have been made to maintain the frequencies and mode shapes of the original model configuration, the changes in pylon mass properties have had an impact on WRATS frequencies and mode shapes. These changes are sufficient enough to warrant testing of the WRATS model to re-establish its baseline stability boundaries.

This paper will present experimental results from recent testing of the WRATS model in the TDT which define the whirl-flutter stability boundaries for the current model configuration. The impact of compressibility effects on these boundaries will be addressed by testing the model in a heavy gas test medium. Since the WRATS gimbaled, stiff in-plane hub possesses a coning flexure, a limited parametric study will be presented showing the effects of the variation of pitch-flap coupling and control system stiffness on the whirl-flutter stability boundaries of a flexured hub. Until now, these effects had only been determined experimentally for the rigid hub JVX configuration.

TEST APPARATUS

Wind Tunnel Description

The NASA-Langley Transonic Dynamics Tunnel is a closed-circuit, continuous-flow, variable-pressure wind tunnel with a 16-ft square test section with cropped corners and several features that make it an ideal facility for conducting tests of aeroelastically-scaled wind-tunnel models (Ref. 19). The TDT can be operated up to Mach 1.2 at pressures from near vacuum to atmospheric and in either air or heavy gas (R-134a) test mediums. Due to the high-risk nature of aeroelastic model testing, several unique features of the TDT have been specifically designed to reduce risk so as to protect the model from destruction and also protect the facility from damage due to model debris. These features include a bypass valve system which quickly decreases airspeed in the test section in the event of an aeroelastic instability, large control room windows for viewing models in the test section, and a tunnel drive fan protection screen designed to prevent model debris from damaging the fan blades. Whirl-flutter testing at the TDT is typically conducted at atmospheric pressures in air or at reduced pressures in R-134a gas such that sea-level air density is attained.

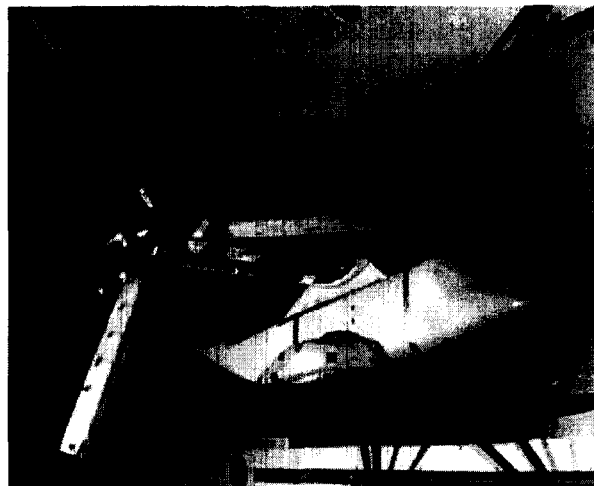


Figure 1: WRATS wind-tunnel model in TDT.

Model Description

The WRATS model is a semispan 1/5-size aeroelastically-scaled tiltrotor model that is a derivative of the JVX/V-22 aeroelastic model designed and built by BHTI described in Ref. 11 and is shown mounted in the TDT test section in Fig. 1. The WRATS model possesses an aeroelastically-scaled (stiffness, mass, and shape) wing and rotor system, a dynamically-scaled (mass and shape) pylon, and a geometrically-scaled (shape only) fuselage which together were designed to match Froude, Lock, and Strouhal numbers when operating in air, and Froude, Lock, Strouhal, and blade Mach numbers when operating in a heavy gas test medium at reduced pressures. The wing structure consists of a composite box-beam spar with aluminum stiffeners to which aerodynamic panels and support structure for the transmission drive shaft and flaperons are attached. The wing is cantilevered to a truss-mounted "splitter plate" which places the rotor near the tunnel centerline and reduces wall boundary layer effects. The baseline pylon hardware consists of an 84-deg gearbox to accommodate pylon tilting, a transmission and mast, simulated infrared suppressor and engine weights, and built-up frame with an aerodynamic fairing. The original electro-mechanically actuated control system was replaced with a hydraulically-actuated control system for the purpose of supporting active controls research. The transmission, gear-box, and mast components are essentially rigid over the range of model frequencies of interest.

The pylon is mounted to the wing at the conversion axis and is free to rotate about this axis for testing in both hover and cruise-flight modes. A downstop spring also attaches the pylon to the wing and simulates the stiffness of the pylon conversion actuator in the locked and

unlocked configurations, which are referred to as the on- and off-downstop configurations. During pylon conversion from hover to cruise flight, the pylon possesses the stiffness of the conversion actuator only. When the pylon is fully converted to cruise flight mode, the pylon is locked onto the downstop which allows less pylon/wing flexibility. The pylon downstop spring stiffness has a large influence on the separation of the wing beam and torsion natural frequencies and the shapes of the corresponding modes, and thus has a major effect on whirl-flutter stability.

The stiff in-plane, 7.6-ft diameter, 3-bladed rotor system consists of aeroelastically-scaled rotor blades attached to a gimbal hub by a composite flexure that allows rotor coning under load and includes 2.5 degrees of precone. The hub flexures contain pitch bearings at each outboard end to allow the blade cuffs to freely rotate when trailing-edge pitch links are translated up or down by the swashplate. The rotor can be powered by a 19-HP electric motor for hover testing or it can windmill in cruise-flight mode in the wind tunnel. To reduce transient blade flapping and avoid a flap-lag instability, the rotor pitch-flap coupling, or δ_3 , for the baseline WRATS model is -15 degrees. For positive δ_3 , blade pitch decreases as the blade flaps up. The scaled rotor blades are highly twisted, with a non-linear twist distribution (nose-down) of 47.5 degrees from root to tip.

The WRATS model is highly instrumented to provide loads, stability, and rotor dynamics information. Such instrumentation includes pylon and wing accelerometers; blade, wing, mast, pitch link, and hub loads via strain gages; rotor flapping via an angular displacement transducer; and swashplate position and orientation via translational displacement transducers. However, for the purpose of discussing whirl-flutter stability test results, only the wing bending and torsion moment strain gage data will be presented. The wing bending loads are measured by three full-bridge strain gages that consist of beamwise and chordwise gages located 17 inches from the wing root and a wing torsion strain gage bridge located 22 inches from the wing root.

Model Vibration Characteristics

A ground vibration test (GVT) was conducted with the model cantilevered to a backstop prior to testing in the TDT. Responses were measured at four locations in the pylon using bi-axial and tri-axial piezoresistive accelerometers and force inputs were measured using piezoelectric force transducers. A commercial data acquisition system and modal analysis software package were used to acquire and analyze the test data to determine the natural frequencies and mode shapes of the wing and pylon structure.

The model was tested in both the on-downstop and off-downstop configurations with the blades replaced with simulated blade weights and the gimbal flapping and rotor rotation locked out. Pylon accelerometer responses were measured while independent random force inputs were applied to the model at the trailing edge of the wing tip in the beamwise and chordwise directions to excite the fundamental wing/pylon modes of vibration consisting of beam, chord, and torsion modes, as well as the pylon yaw mode. Fig. 2 shows the WRATS model during ground vibration testing with the pylon and wing aerodynamic panels removed for clarity and identifies the coordinate system, response accelerometer locations, and excitation shakers.

Table 1 and Figs. 3 through 5 present ground vibration test results for the WRATS model in the off-downstop configuration. Results for the on-downstop configuration of the WRATS model are presented in Table 2 and Figs. 6 through 8. Mode shape data in Tables 1 and 2 represent interpolated mode shapes at the rotor hub. For the off-downstop configuration, Fig. 3 illustrates the wing beam mode which exhibits both vertical and pitch motion of the pylon and Fig. 4 illustrates the wing chord motion which exhibits axial, yaw, and pitch motion of the pylon. Figure 5 illustrates the wing torsion mode as measured for the off-downstop configuration. Figure 6 illustrates the wing beam mode for the on-downstop configuration and reveals less pylon pitch motion when compared to the corresponding mode for the off-downstop configuration (Fig. 3). Since the wing beam mode is the dominant participant in whirl-flutter for this model's characteristics, the decreased pitch motion will be shown to result in an increased stability boundary for the on-downstop configuration. For the on-downstop configuration, Fig. 7 shows the wing chord mode and Fig. 8 shows the wing torsion mode. The pylon yaw mode is presented in Tables 1 and 2, and can be described as a second wing chord mode.

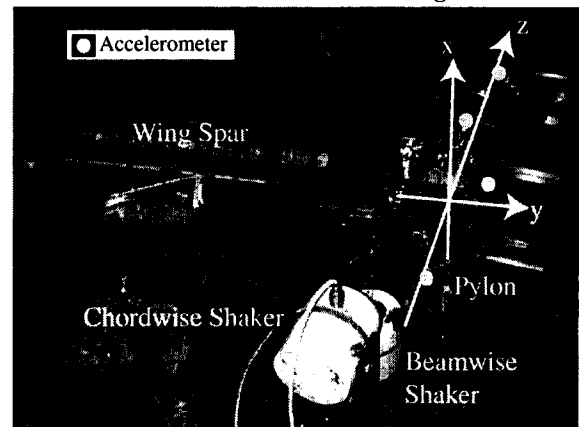


Figure 2: WRATS model during ground vibration testing.

Table 1: WRATS off-downstop interpolated mode shapes at the rotor hub

Mode	Frequency, Hz	Damping, %	x, in	y, in	z, in	θ_x, rad	θ_y, rad
Wing Beam	5.43	1.5	3.69	0.01	0.14	0.016	0.102
Wing Chord	8.11	1.28	0.28	-1.62	2.58	0.083	0.068
Wing Torsion	10.54	1.51	-2.25	-0.43	0.39	0.054	-0.251
Pylon Yaw	14.77	3.25	1.31	-3.36	0.12	0.072	-0.002

Table 2: WRATS on-downstop interpolated mode shapes at the rotor hub

Mode	Frequency, Hz	Damping, %	x, in	y, in	z, in	θ_x, rad	θ_y, rad
Wing Beam	5.83	1.39	3.43	0.10	0.03	0.016	0.067
Wing Chord	8.67	1.41	0.28	-0.99	2.13	0.058	0.043
Wing Torsion	12.02	2.62	2.65	0.21	-0.34	-0.041	0.261
Pylon Yaw	19.43	4.85	0.09	3.57	0.57	-0.170	-0.013

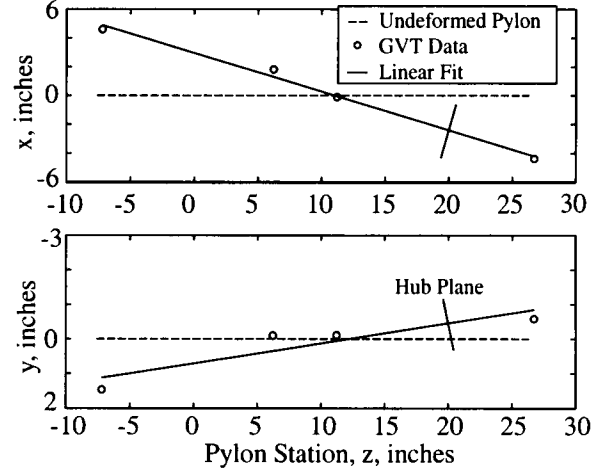
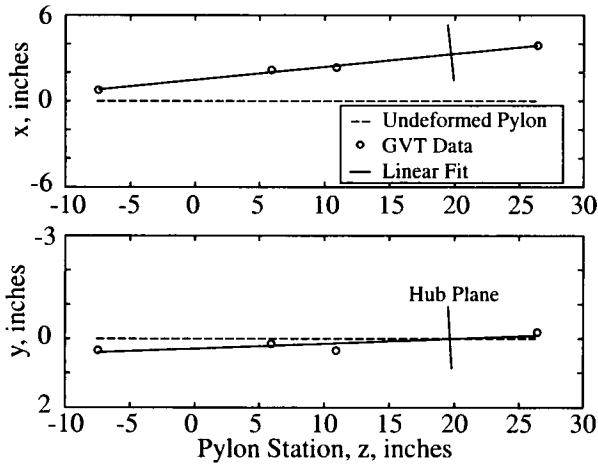


Figure 3: Off-downstop wing beam mode shape (5.43 Hz).

Figure 5: Off-downstop wing torsion mode shape (10.54 Hz).

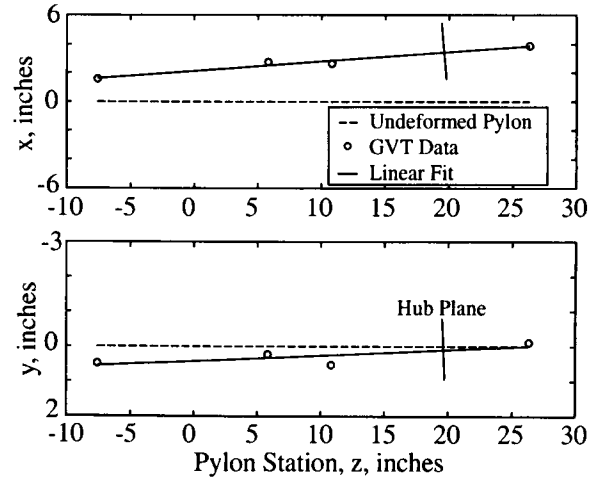
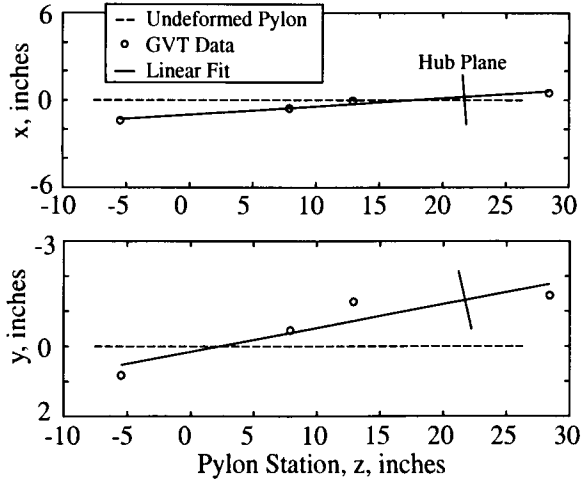


Figure 4: Off-downstop wing chord mode shape (8.11 Hz).

Figure 6: On-downstop wing beam mode shape (5.83 Hz).

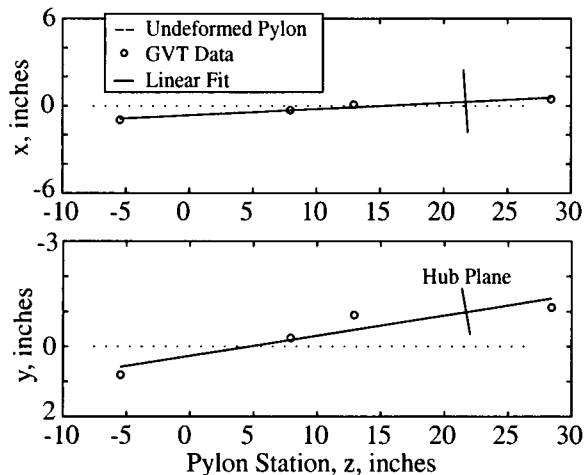


Figure 7: On-downstop wing chord mode shape (8.67 Hz).

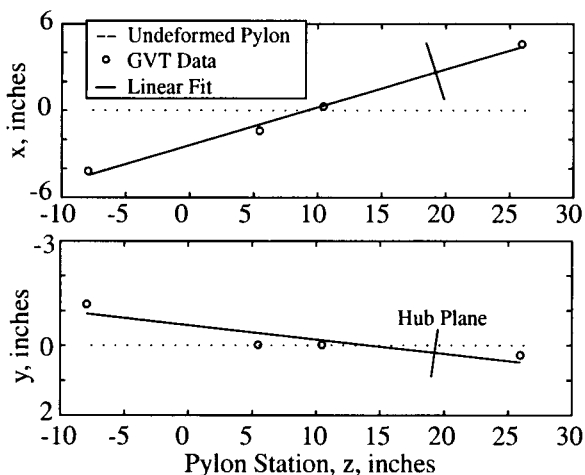


Figure 8: On-downstop wing torsion mode shape (12.02 Hz).

TEST PROCEDURES

Whirl-flutter testing is conducted by experimentally measuring the subcritical damping and frequencies of the fundamental pylon/wing modes up to the airspeed at which the model becomes neutrally stable or unstable, i.e. exhibits zero or negative damping when excited. Damping is determined by exciting the proper mode and analyzing the appropriate wing strain gage time history.

Because of the high-risk nature of whirl-flutter testing, WRATS test engineers rely on several means to protect the model from overloading and destruction. As a whirl-flutter instability is approached, careful attention is paid to readouts of wing bending loads and the model is closely watched at all times. At the first visual indication of a steady, large amplitude pylon response (neutrally stable)

or a growing pylon response (unstable), rotor speed is reduced, which is usually enough to stabilize the model. If the pylon motion becomes significant or if reducing rotor speed has little effect, the TDT's bypass valves are triggered, which greatly reduces tunnel airspeed and stabilizes the model.

Prior to whirl-flutter testing, the rotor is tracked such that each blade tip travels in the same plane and is balanced such that the center of mass of the rotor is at, or very near to, the center of rotation to minimize 1/rev vibrations. Initial tracking is usually completed at reduced rotor speeds, depending on the amount of rotor unbalance, and is visually determined by darkening the model area and strobing the blade tips at 3/rev such that all three appear overlaid at approximately the same position. Blade tracking is adjusted by making minute incremental changes to blade root pitch. When rotor tracking is acceptable, balancing the rotor can begin. Based on observations of pylon vibration magnitude and phase data, lead tape is distributed to each blade tip leading edge to balance the rotor until the pylon vibration magnitude is within a threshold range (usually $< 0.05g$). At that point, 100% rotor speed can be attained and the rotor tracking re-checked. Tracking and balancing is first accomplished in the hover configuration in powered mode using an electric motor to drive the rotor and is then fine-tuned during initial wind-tunnel runs with the rotor windmilling.

Following tracking and balancing of the rotor, whirl-flutter testing is conducted at constant tunnel airspeeds with the rotor windmilling in a "trimmed" state. The rotor is trimmed by a pilot using collective pitch to maintain a desired rotor speed and cyclic pitch to zero rotor flapping. When the rotor is satisfactorily trimmed, the desired wing/pylon mode is excited (using methods described in the next paragraph) and the free decay response of the model is measured from which the damping at the current airspeed and rotor rotational speed combination can be determined. Five or more repeat data records are acquired to reduce any bias in the measurements. Rotor rotational speed is then decreased by 10-15 RPM, tunnel airspeed is increased to the next condition, and rotor rotational speed is slowly increased back to the nominal speed while the model is monitored for an instability. Once at a trimmed condition at the new tunnel airspeed, data are recorded and the process is repeated until an instability is observed, damping is sufficiently small (usually $< 0.5\%$ critical), or the maximum rotor collective pitch is reached.

In previous WRATS tests in the TDT, pulse jets emitting a heavy gas were used to excite the WRATS model to provide the transient response data used to determine damping. This method was inefficient due to time required to pressurize the pulse system and because testing

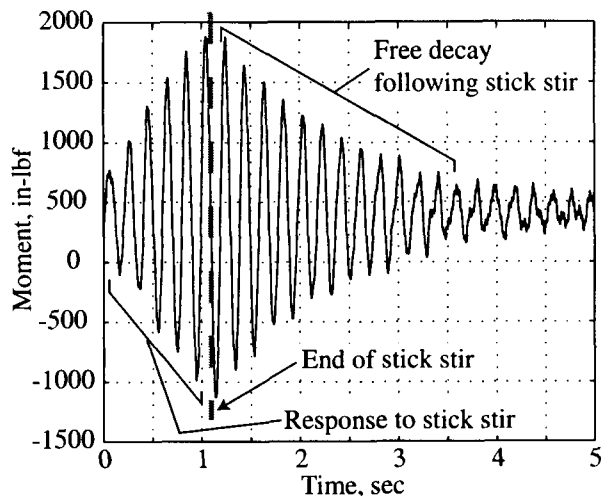


Figure 9: Typical wing beam bending moment time history for damping determination.

had to be stopped periodically to replenish the gas system. A new and very efficient method of exciting the WRATS model is now used which takes advantage of the high-bandwidth hydraulic actuators that were installed as part of an active swashplate control system. Cyclic or collective pitch “stick stirs” are applied to the swashplate at a specified frequency to excite a wing/pylon mode. These sinusoidal excitation commands are added with the steady pilot control commands before being sent to the actuators. In addition to amplitude and frequency of the stick stir, the length and ramp-up rate of the stick stir is varied as a means of controlling the degree of model excitation. Control of the stir is integrated into the WRATS data acquisition system’s graphical user interface (GUI) to facilitate the exciting of the model and the recording of data. When the model excitation is sufficient, a kill-switch is engaged that quickly ramps the stick stir to zero and allows the free decay of the model oscillation, as illustrated in Fig. 9.

The excitation and free decay of the model is recorded by the WRATS data acquisition system (DAS) which is a 64-channel multiplexed A/D system used to acquire and analyze model data. In addition to FFT and harmonic analysis capabilities, the WRATS DAS employs the moving block and log decrement method for the determination of subcritical damping from the recorded time histories. The moving block method, which is described in Refs. 20 and 21, is quite effective at determining the damping of a specific mode in the presence of other modes and signal noise. By analyzing the appropriate wing strain gage response, the damping of the mode of interest is easily and quickly determined. Using the GUI-driven stick stir and moving block methods, wind-tunnel test time is used very efficiently.

TEST RESULTS

Experimental damping and frequency measurements from the current WRATS configuration have been made in order to define its whirl-flutter stability boundaries. Results will be presented as graphs of modal damping and frequency versus tunnel airspeed. Graphs of wing beam mode damping indicate the point of zero damping (whirl-flutter boundary) for a given configuration. For all such figures presented, error bars indicate the standard deviation of repeat data points for a particular airspeed and configuration, and markers indicate the average of those same points. The standard deviation shown is primarily a reflection of wind-tunnel turbulence. Curve fits have been applied through the averages at each airspeed and extrapolated, where appropriate, to zero wing beam mode damping to indicate the neutral whirl-flutter stability airspeed. For the WRATS model, the wing beam bending mode is the primary participant and indicator of whirl flutter and therefore warrants the greatest attention for this discussion. Typically, five or more data points have been acquired at each airspeed for averaging purposes to lessen the effects of tunnel turbulence. Past whirl-flutter tests have not typically acquired as many repeat points (sometimes as few as one or two). A greater number of repeat points corresponds to higher confidence in the test results and the “averaging out” of bias effects. The greater number of repeat data points acquired during recent WRATS tests is attributable to the stick stir method of excitation.

The model was tested in the on- and off-downstop configurations at rotor rotational speeds of 888 revolutions per minute (RPM), 770 RPM, and 742 RPM. The 888 RPM condition represents hover rotor speed, 742 RPM is the cruise flight rotor speed, and 770 RPM was a compromise to 742 RPM because of the proximity of the model’s torsional frequency to 742 RPM in the on-downstop configuration. The effect of pitch-flap coupling, control system stiffness, and test medium (R-134a versus air) on system damping was determined for the model configurations and test conditions discussed above.

Baseline Stability Boundaries

Figure 10 shows the wing beam mode damping and frequency trends versus tunnel airspeed for the off-downstop pylon stiffness configuration and steady rotor speeds of 742 and 888 RPM. In Fig. 10, wing beam mode damping is shown to be zero (neutrally stable) at 88 knots for 888 RPM and is extrapolated to zero at 142 knots for 742 RPM for this configuration. The wing chord mode (Fig. 11) is highly damped for all airspeeds within the stable range of whirl flutter and will not be discussed further. Figures 10 and 11 show the decrease in wing beam and chord frequencies as tunnel airspeed is increased.

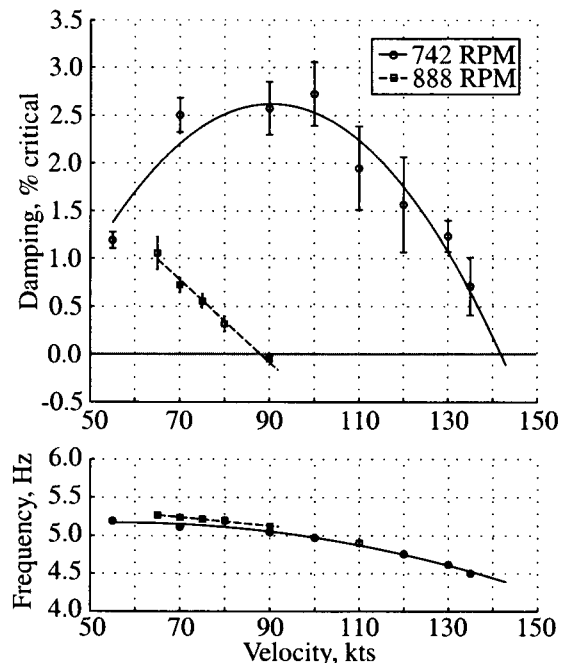


Figure 10: Off-downstop wing beam damping and frequency versus tunnel airspeed for the baseline configuration.

The model wing beam damping and frequency versus tunnel airspeed for the on-downstop configuration are presented in Fig. 12 for 770 and 888 RPM. The projected whirl-flutter instability conditions for this configuration are shown to be 155 knots for 888 RPM and 187 knots for 770 RPM. Figure 13 summarizes the current WRATS stability boundaries for the on- and off-downstop configurations. The observed increased stability of the on-downstop configuration is due to the decreased participation of pylon pitch motion in the wing beam mode. The on-downstop configuration represents a pylon locked on the downstop which is more stiff when compared to the off-downstop configuration that represents only the pylon conversion actuator stiffness. This increased pylon mount stiffness results in greater separation of the wing beam and torsion modes, less participation of pylon pitch motion in the beam mode, and therefore a higher whirl-flutter stability boundary.

Effect of Reduced Control System Stiffness on Whirl-Flutter Stability

In Refs. 12 and 13, the blade torsion dynamics associated with positive pitch-lag coupling (lag back, pitch up) were analytically shown to have a destabilizing influence on whirl-flutter stability boundaries for a rigid rotor hub and the pitch-lag coupling was shown to be affected by control system stiffness and rotor coning. Since the

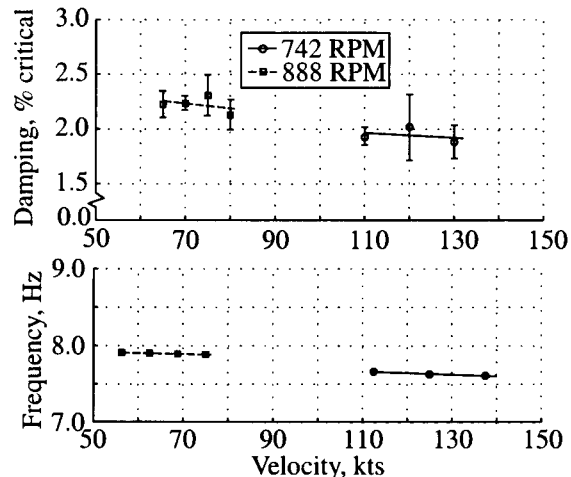


Figure 11: Off-downstop wing chord damping and frequency versus tunnel airspeed for the baseline configuration.

presence of a flexured hub has an effect on the coning characteristics of a tiltrotor, results from previous control system stiffness studies for a rigid hub can be expected to be different for the present WRATS coning-flexured hub configuration. In this section, the effects of control system stiffness on whirl-flutter stability for a flexured-hub tiltrotor configuration will be presented. Appendix A discusses in detail the pitch-lag dynamics of a rigid and flexured hub tiltrotor.

To assess the effects of control system stiffness on stability, modified pitch horns which connect to the pitch links and blade cuffs were manufactured with reduced stiffness while maintaining the identical geometry of the baseline pitch horns. The control system stiffness (C_k) was measured with the model in the hover configuration, blades off, and with nominal hydraulic system pressure. Figure 14 shows the results of these measurements. The softened pitch horns are shown to reduce the control system stiffness by more than 50 percent which, according to past rigid hub analyses, should increase the degree of pitch-lag coupling and reduce whirl-flutter stability. The rigid-body pitch mode of the blade on the hub due to control system flexibility was measured to be 95.6 Hz for the baseline control system stiffness.

Experimental results in Fig. 15 present the wing beam mode damping for the baseline (previously presented in Fig. 10) and soft control system for the model in the off-downstop configuration at 742 and 888 RPM. Wing beam mode frequency is also presented in Fig. 15 for the soft control system. The reduced control system stiffness is shown to have little effect on wing beam mode damping at 742 RPM while an increase in beam damping is observed at 888 RPM. The latter behavior is contrary to published analytical (Refs. 12 and 13) and experimental (Refs. 10

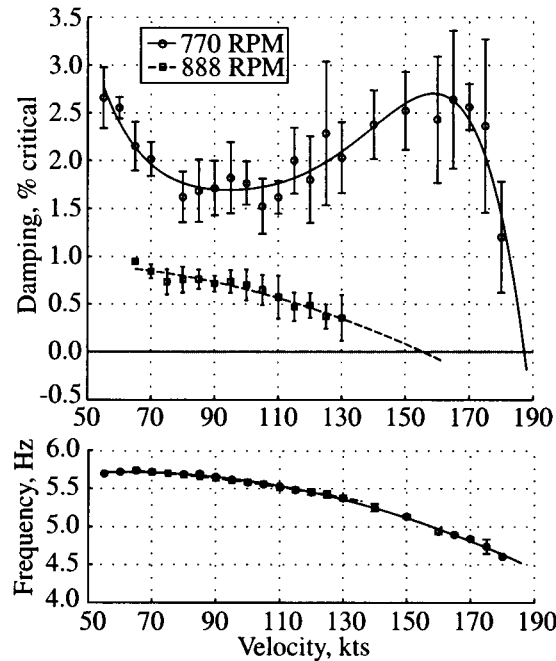


Figure 12: On-downstop wing beam mode damping and frequency versus tunnel airspeed for the baseline configuration.

and 11) results for a rigid hub. For the on-downstop model configuration, Fig. 16 presents wing beam mode damping and frequency for the baseline (previously presented in Fig. 12) and soft control system configuration. In Fig. 16, the control system stiffness is not shown to have a significant impact on wing beam mode damping at either 770 or 888 RPM for the on-downstop configuration. Testing at 770 RPM for this configuration was halted at 130 knots due to the upper collective limit for the soft control system. While past studies have shown that decreasing control system stiffness has a destabilizing effect on the stability of a rigid hub, the results of the present study suggest that the effect of control system stiffness on pitch-lag coupling and whirl-flutter stability is greatly reduced by the presence of a flexured hub.

Effect of Pitch-Flap Coupling on Whirl-Flutter Stability

Pitch-flap coupling is an effective means of reducing the flapping response of a tiltrotor without adversely affecting blade loads. The use of pitch-flap coupling moves the flapping natural frequency away from the resonant condition of a gimballed rotor with zero hinge offset. This kinematic coupling is applied through the orientation of the blade pitch link with respect to the flapping hinge or hub gimbal and causes an increase in blade pitch as the blade flaps up for positive pitch-flap coupling (negative δ_3). This incremental change in blade pitch due to blade

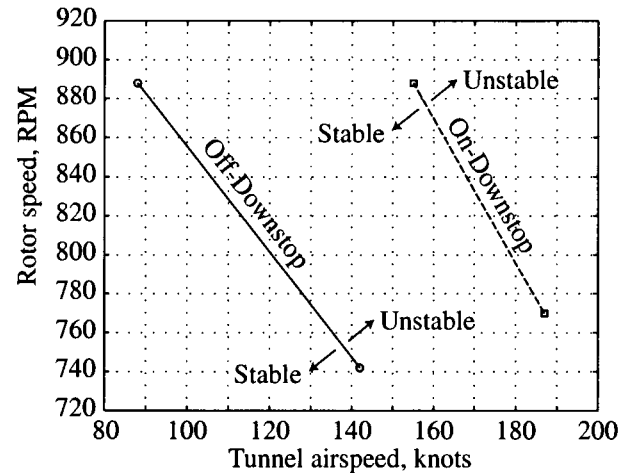


Figure 13: Whirl-flutter stability boundaries for the baseline configuration.

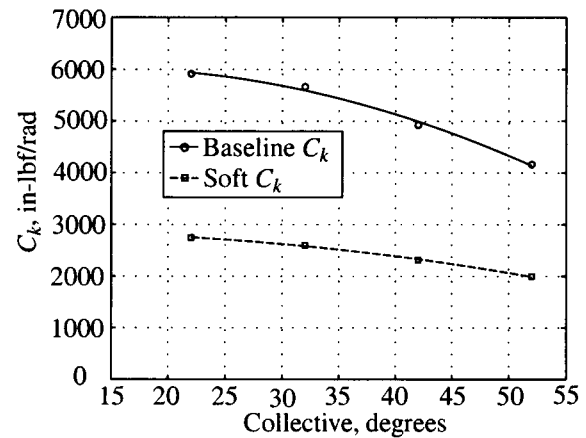


Figure 14: Baseline and soft control system stiffness versus collective angle.

flapping causes an aerodynamic flapping moment which changes the flapping natural frequency without changing the stiffness of the blade flapping restraint. While reducing the flapping response of a tiltrotor during maneuvers, positive and negative magnitudes of δ_3 are destabilizing for whirl-flutter stability and too much positive δ_3 can lead to blade flap-lag instability (Ref. 22).

The effective δ_3 of the rotor system is reduced due to the presence of the flexured hub which affects the rotor gimbal mode by providing an additional virtual flapping hinge between the gimbal and the pitch bearing. This effect is relatively easy to quantify for an offset coning-hinge configuration, but is more difficult for a flexured hub. This effect has not been previously investigated for a gimballed, stiff in-plane, flexured hub.

For the present investigation, the WRATS δ_3 was changed from its baseline value of $\delta_3 = -15^\circ$ to $\delta_3 = -45^\circ$

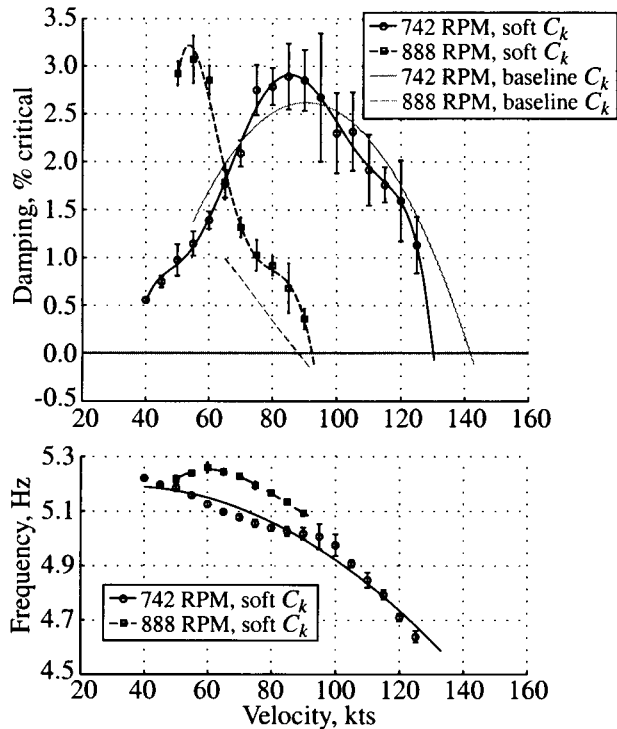


Figure 15: Off-downstop wing beam mode damping and frequency versus tunnel airspeed for the soft and baseline control system.

using blade cuff pitch-horns and a rotating system swash-plate which moved the location of the pitch link with respect to the gimbal center. Figure 17 illustrates the effect that rotor pitch-flap coupling has on whirl-flutter stability. In this figure, experimental wing beam damping results from the WRATS model in the $\delta_3 = -45^\circ$ configuration are compared to the baseline damping results from Fig. 12. In addition to damping, Fig. 17 presents the wing beam mode frequency versus tunnel airspeed for rotor speeds of 770 and 888 RPM for the $\delta_3 = -45^\circ$ configuration. Figure 18 presents the comparison of the baseline ($\delta_3 = -15^\circ$) whirl-flutter boundary in air to the $\delta_3 = -45^\circ$ boundary. These results suggest that the destabilizing effects of pitch-flap coupling are not significantly affected by the flexured hub even though, when compared to a rigid hub, the flexured hub tends to reduce the effective pitch-flap coupling due to the presence of the additional virtual flapping hinge.

Effect of Test Medium on Whirl-Flutter Stability

The effects of compressibility on WRATS whirl-flutter stability was investigated by testing in a heavy gas medium (R-134a) at a reduced pressure such that the density of air at sea level is matched while the test medium speed of sound is approximately one half that of air. The reduced test medium speed of sound in R-134a results in a

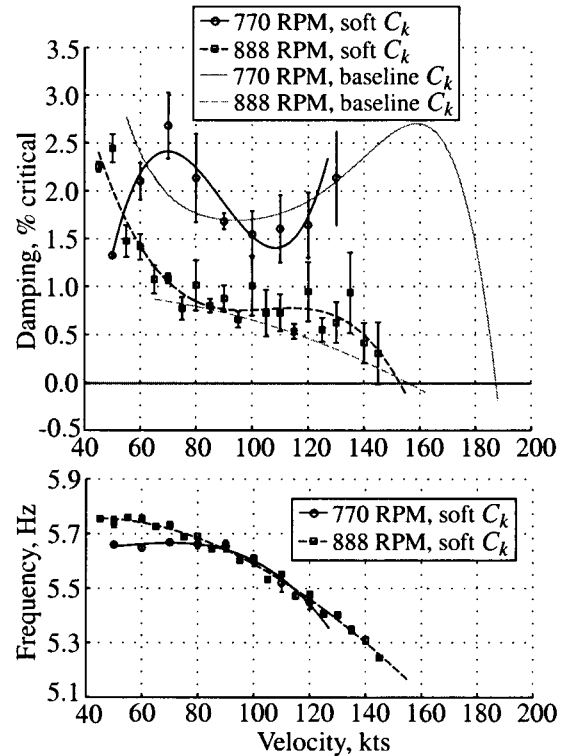


Figure 16: On-downstop wing beam mode damping and frequency versus tunnel airspeed for the soft and baseline control system.

higher Mach number at any blade radial station than that in an air test medium for a given rotor speed. For example, at 888 RPM the tip Mach number in air is 0.32 and is 0.65 in R-134a. Since the blade airfoil lift curve slope is proportional to Mach number, larger blade aerodynamic forces result when tests are conducted in R-134a. These larger aerodynamic forces have a destabilizing effect on whirl-flutter stability. This trend is indicated in Fig. 19 which compares WRATS wing beam mode damping in air (previously presented in Fig. 12) and R-134a for the on-downstop baseline model at 770 and 888 RPM. Figure 19 also presents the wing beam mode frequency versus tunnel airspeed for results in R-134a. Figure 18 compares the baseline whirl-flutter boundary in air to the baseline boundary in R-134a and shows a 12 knot decrease in stability at 770 RPM and a 35 knot decrease at 888 RPM for R-134a. Results indicate that testing in R-134a, and thus matching full-scale tip Mach number, has a destabilizing effect, which demonstrates that whirl-flutter stability boundaries in air are unconservative.

CONCLUSIONS

The baseline whirl-flutter stability boundaries of the WRATS model with modified pylon properties have been

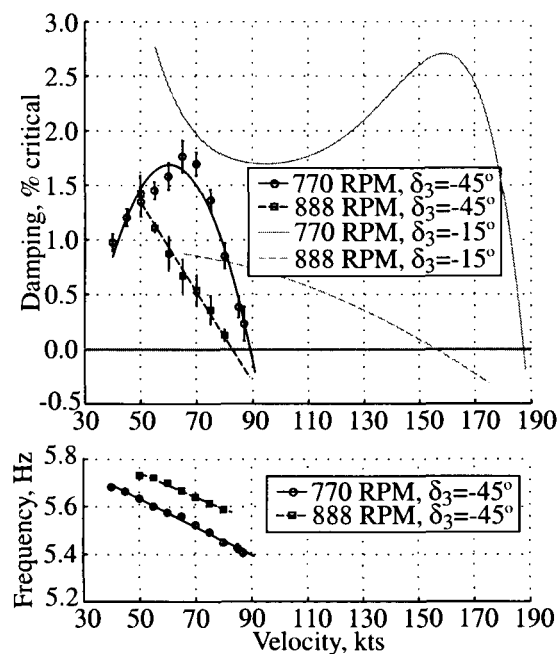


Figure 17: On-downstop wing beam mode damping and frequency versus tunnel airspeed for $\delta_3 = -45^\circ$ and $\delta_3 = -15^\circ$.

identified for the on- and off-downstop pylon stiffness configurations at both cruise and hover rotor speed conditions during testing at the NASA-Langley Transonic Dynamics Tunnel. The use of swashplate stick stirs to excite the model modes of vibration greatly improved the speed and efficiency of whirl-flutter testing over previous methods used at the TDT.

A parametric study was undertaken to provide experimental data on the effect of several parameters on the whirl-flutter stability of the current WRATS tiltrotor model. This is the first parametric study of the effect of control system stiffness and pitch-flap coupling on a flexured rotor hub. It is hoped that this study, on a well-documented aeroelastically-scaled tiltrotor model, will provide valuable data for stability analysis correlation and comparison to future advanced configurations. The following conclusions were noted:

1. Reducing control system stiffness by more than 50 percent did not have a significant impact on damping and stability of the WRATS model with a flexured, stiff in-plane hub for most model configurations. At one configuration, off-downstop and 888 RPM, the damping was shown to be increased by the reduction in control system stiffness, which is contrary to previous analytical and experimental studies. While decreasing control system stiffness has been shown to have a significant destabilizing effect on the stability of a rigid hub, the results of the present study suggest

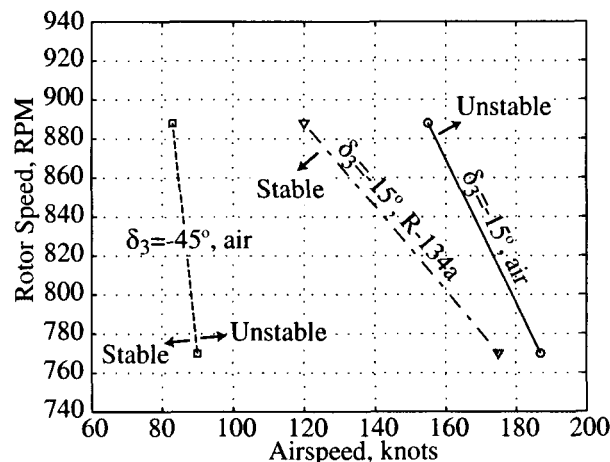


Figure 18: On-downstop whirl-flutter boundaries for δ_3 and test medium variations.

that the detrimental effect of control system stiffness on blade pitch-lag coupling and whirl-flutter stability is greatly reduced by the presence of a flexured hub.

2. Increasing the magnitude of pitch-flap coupling from $\delta_3 = -15^\circ$ to $\delta_3 = -45^\circ$ significantly reduced the on-downstop whirl-flutter stability boundary. These results suggest that the destabilizing effects of pitch-flap coupling are not significantly affected by the flexured hub even though, when compared to a rigid hub, the flexured hub tends to reduce the effective pitch-flap coupling due to the presence of the additional virtual flapping hinge of the flexure.
3. Results indicate that testing in R-134a has a destabilizing effect, which demonstrates that whirl-flutter stability boundaries in air are unconservative. Using an R-134a test medium, WRATS on-downstop stability was decreased by 12 knots at 770 RPM and by 35 knots at 888 RPM when compared to results for the baseline configuration in air. Testing in heavy gas (R-134a) matches the full scale tip Mach number for the WRATS model and thereby accounts for compressibility effects that increase the blade airfoil lift curve slope, which increase the destabilizing aerodynamic loads generated by rotor precession.

APPENDIX A

ORIGIN OF PITCH-LAG COUPLING

Blade torsion dynamics associated with pitch-lag coupling have a destabilizing effect on whirl-flutter stability boundaries and this effect has been shown analytically in Refs. 12 and 13. Blade pitch-lag coupling is affected by

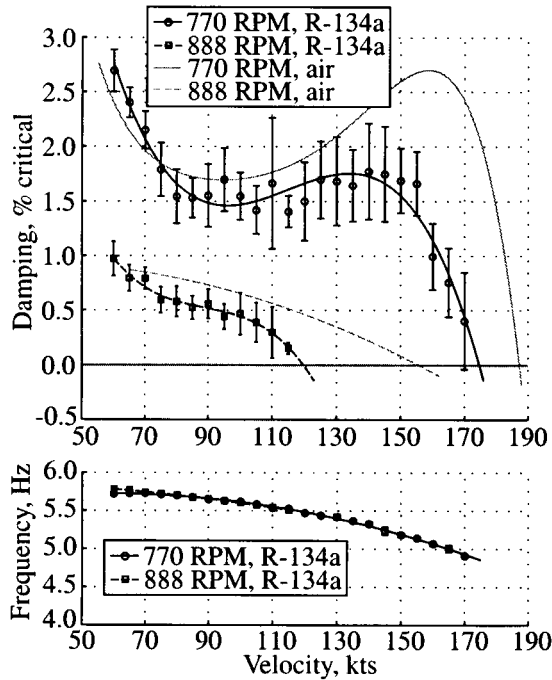


Figure 19: On-downstop wing beam damping and frequency versus tunnel airspeed in a R-134a and air test medium.

control system stiffness and rotor precone. Rotor precone is a design solution which alleviates the large blade root bending moments of a high disk loading tiltrotor by balancing the moment due to centrifugal force and the aerodynamic flapping moment under hover conditions. This is illustrated in Fig. 20a where β_p is the precone angle, r is the blade radial station, dL is the incremental blade lift, and $\Omega^2 r dm$ is the incremental centrifugal force. However, at cruise flight conditions, the blade aerodynamic flapping moment is greatly reduced while the moment due to centrifugal loads is reduced by a much smaller degree, which results in a net flap moment. This net flap moment, due to non-ideal precone in cruise flight, has a component about the blade pitch axis as the blade lags back as shown in Fig. 20b where $d\eta$ represents blade lag angle. This is the origin of positive pitch-lag coupling (lag back, pitch up) which is destabilizing to tiltrotor whirl flutter. To reduce the magnitude of the pitch-lag coupling and therefore improve whirl-flutter stability, the flexured hub is designed to allow the rotor to “flatten out” under centrifugal loads in cruise flight and reduce rotor coning by the angle β_h as shown in Fig. 20c. This reduction in rotor coning effectively reduces the torsional moment about the inboard blade sections for a given lag angle as shown in Fig. 20d and therefore reduces the blade pitch-lag coupling.

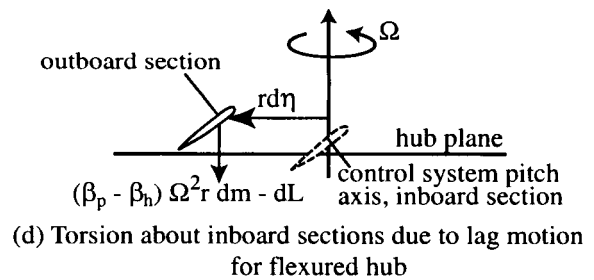
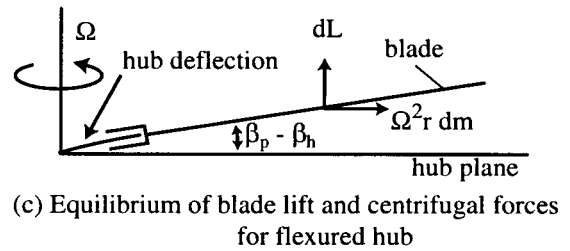
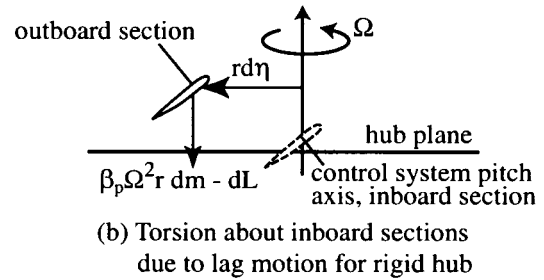
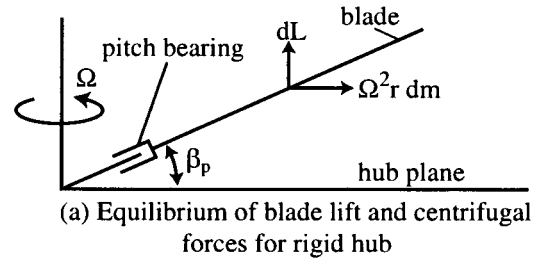


Figure 20: Origin of blade pitch-lag coupling and the impact of a flexured hub.

REFERENCES

1. Houbolt, J.C. and Reed, W.H., "Propeller-Nacelle Whirl-Flutter". *Journal of the Aerospace Sciences*, Volume 29, No. 3, 1962.
2. Reed, W.H., "Propeller-Rotor Whirl-Flutter: A State of the Art Review". *Journal of Sound and Vibration*, Volume 4, pp. 526-544, 1966.
3. Kvaternik, R.G., "Studies in Tilt-Rotor VTOL Aircraft Aeroelasticity". Ph.D. Dissertation, Case Western University, June 1973.
4. Hall, E.W.Jr., "Prop-Rotor Stability at High Advance Ratios". *Journal of the American Helicopter Society*, June 1966.
5. Edenborough, H.K., "Investigation of Tilt-rotor VTOL Aircraft Rotor-Pylon Stability". *Journal of Aircraft*, Volume 5, No. 6, March-April, 1968.
6. Gaffey, T.M., Yen, J.G., and Kvaternik, R.G., "Analysis and Model Tests of the Proprotor Dynamics of a Tilt-Proprotor VTOL Aircraft". Presented at the Air Force V/STOL Technology and Planning Conference, Las Vegas, Nevada, September 23-25, 1969.
7. Kvaternik, R.G., "A Review of Some Tilt-Rotor Aeroelastic Research at NASA-Langley". *Journal of Aircraft*, Vol. 13, No. 5, May 1976.
8. Kvaternik, R.G., "Experimental and Analytical Studies in Tilt-Rotor Aeroelasticity". Presented at the AHS/NASA Ames Specialists' Meeting on Rotorcraft Dynamics, February 13-15, 1974.
9. Kvaternik, R.G. and Kohn, J.S., "An Experimental and Analytical Investigation of Proprotor whirl-flutter". NASA Technical Paper 1047, December, 1977.
10. Popelka, D., Sheffler, M., and Bilger, J., "Correlation of Test and Analysis for the 1/5-Scale V-22 Aeroelastic Model". *Journal of the American Helicopter Society*, Volume 32, No. 2, April 1987.
11. Settle, T.B. and Kidd, D.L., "Evolution and Test History of the V-22 0.2-Scale Aeroelastic Model". American Helicopter Society National Specialists' Meeting on Rotorcraft Dynamics, Arlington, Texas, November 1989.
12. Johnson, W., "Analytical Modeling Requirements for Tiltrotor Proprotor Aircraft Dynamics". NASA TN D-8013, July 1975.
13. Nixon, M.W., "Aeroelastic Response and Stability of Tiltrotors with Elastically-Coupled Composite Rotor Blades". Ph.D. Dissertation, University of Maryland, 1993.
14. Corso, L.M., Popelka, D.A., and Nixon, M.W., "Design, Analysis, and Test of a Composite Tailored Tiltrotor Wing". American Helicopter Society 53rd Annual Forum, Virginia Beach, VA, April 1997.
15. Nixon, M.W., Piatak, D.J., Corso, L.M., and Popelka, D.A., "Aeroelastic Tailoring for Stability Augmentation and Performance Enhancements of Tiltrotor Aircraft". American Helicopter Society 55th Annual Forum, Montreal, Quebec, Canada, May 25-27, 1999.
16. Settle, T.B. and Nixon, M.W., "MAVSS Control of an Active Flaperon for Tiltrotor Vibration Reduction". American Helicopter Society 53rd Annual Forum, Virginia Beach, VA, April 1997.
17. Nixon, M.W., Kvaternik, R.G., and Settle, T.B., "Tiltrotor Vibration Reduction Through Higher Harmonic Control". American Helicopter Society 53rd Annual Forum, Virginia Beach, VA, April 1997.
18. Nixon, M.W., Langston, C.W., Singleton, J.D., Piatak, D.J., Kvaternik, R.G., Corso, L.M., and Brown, R., "Aeroelastic Stability of a Soft-Inplane Gimballed Tiltrotor Model in Hover". Presented at the 42nd AIAA/ASME/ASCE/AHS/ASC Structures, Structural Dynamics, and Materials Conference, Seattle Washington, April 16-19, 2001.
19. Cole, S.R. and Garcia, J.L., "Past, Present, and Future Capabilities of the Transonic Dynamics Tunnel from an Aeroelasticity Perspective". Presented at the AIAA Dynamics Specialists Conference, Atlanta, GA, April 5-6, 2000.
20. Hammond, C.E. and Doggett, R.V. Jr., "Determination of Subcritical Damping by Moving Block/Randomdec Applications". NASA Symposium on Flutter Testing Techniques, NASA SP-415, October 1975, pp.59-76.
21. Bousman, W.G. and Winkler, D.J., "Application of the Moving Block Analysis". 22nd Structures, Structural Dynamics, and Materials Conference, AIAA Paper No. 81-0653, April 6-8, 1981.
22. Gaffey, T.M., "The Effect of Positive Pitch-Flap Coupling (Negative δ_3) on Rotor Blade Motion Stability and Flapping". *Journal of the American Helicopter Society*, April 1969.

June 14, 2001

NASA STI Acquisitions DAA Authorization

The following papers (copies enclosed) have been DAA approved as Unclassified, Publicly Available documents:

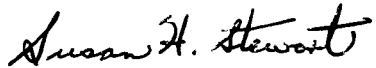
Meeting Presentations:

- 42rd AIAA/ASME/ASCE/AHS/ASC Structure & Structural Dyn..., 4/16-19/2001, Seattle, WA:
B.H. Mason: Coupled Aerodynamic and Structural Sensitivity Analysis of a High-Speed...
M.D. Billings, *et al.*: Impact Test and Simulation of Energy Absorbing Concepts for...
M.C. Reaves, *et al.*: Test Cases for Modeling and Validation of Structures with...
I.S. Raju, *et al.*: Meshless Petrov-Galerkin Method Applied to Axisymmetric Problems.
- 7th AIAA/CEAS Aeroacoustics Conf. 5/28-30/2001, Maastricht, The Netherlands:
M.R. Khorrami, *et al.*: A Novel Approach for Reducing Rotor Tip-Clearance Induced...
F.W. Grosveld, *et al.*: Structural and Acoustic Numerical Modeling of a Curved Composite...
M.G. Jones, *et al.*: Comparison of Two Acoustic Waveguide Methods for Determining...
F. Farassat, *et al.*: The Detection of Radiated Modes From Ducted Fan Engines.
M.R. Khorrami, *et al.*: Time-Accurate Simulations and Acoustic Analysis of Slat Free...
R.H. Thomas, *et al.*: Computational Analysis of a Pylon-Chevron Core Nozzle Interaction.
- American Helicopter Society 57th Annual Forum, 5/9-11/2001, Washington, DC:
K.H. Lyle, *et al.*: Evaluation of Test/Analysis Correlation Methods for Crash Applications.
J. Li, *et al.*: High Fidelity Failure Analysis for a Composite Fuselage Section.
G.B. Murr, *et al.*: Fatigue and Damage Tolerance Analysis of a Hybrid Composite Tapered...
R.G. Kvaternik, *et al.*: An Experimental Evaluation of Generalized Predictive Control...
D.D. Boyd, *et al.*: Analysis of Measured and Predicted Acoustics from an XV-15...
D.A. Piatak, *et al.*: A Wind-Tunnel Parametric Investigation of Tiltrotor Whirl-Flutter...
- NATO/RTO Symposium on Advanced Flow Management, Part A..., 5/7-11/2001, Loen, Norway:
J.M. Brandon, *et al.*: In-Flight Visualization Results of the F-106B with a Vortex Flap.
J.E. Lamar: Cranked Arrow Wing (F-16XL-1) Flight Flow Physics with CFD Predictions...
- Tiltrotor/Runway Independent Aircraft Techn. & Applications..., 3/20-21/2001, Arlington, TX:
B.D. Edwards, *et al.*: NASA/Army/Bell XV-15 Tiltrotor Low-Noise Terminal Area...
- 2nd Int'l Symp. of Atmospheric Reentry Vehicle & Systems, 3/26-29/2001; Acrachon, France:
R. Mitcheltree, *et al.*: An Earth Entry Vehicle for Returning Samples From Mars.
- 10th AIAA/NAL-NASDA-ISAS Int'l Space Planes & Hypersonic..., 4/24-27/2001, Kyoto, Japan:
R.J. Bakos, *et al.*: Hyper-X Mach 10 Engine Flowpath Development: Fifth Entry Test...
D.E. Reubush, *et al.*: Hyper-X Stage Separation - Simulation Development and Results.

Journal Article:

- D.D. Davis, *et al.*: Impact of Ship Emissions on Marine Boundary Layers...(GRL, 2001)
K.H. Rosenlof, *et al.*: Stratospheric Water Vapor Increases Over the Past Half...(GRL, 2001)
R.E. Southward, *et al.*: Reflective and Electrically Conductive Surface...(Prog Organic.. (2001)
P. Yang, *et al.*: Asymptotic Solutions for Optical Properties of Large...(Applied Optics, 2001)
J.F. Meyers, *et al.*: Characterization of Measurement Error Sources...(Meas. Sci. Techn., 2001)

D.R. Ambur, *et al.*: Optimal Design of Grid-Stiffened Panels and Shells...(Comp. Struc., 2001)
A. Tessler, *et al.*: A {1,2}-Order Plate Theory Accounting for Three...(Comp. Struc., 2001)
L.M. Nicholson, *et al.*: Crosslink Density and Molecular Weight Effects on...(Poly. Prep., 2001)



Susan H. Stewart
DAA Representative
NASA Langley Research Center
Mail Stop 196
Hampton, VA 23681-2199

s.h.stewart@larc.nasa.gov
phone: (757) 864-2518
fax: (757) 864-2375